Superfluid helium quantum interference devices (SHeQUIDs): principles and performance



2014 J. Phys.: Conf. Ser. 568 012015

(http://iopscience.iop.org/1742-6596/568/1/012015)

# Superfluid helium quantum interference devices (SHeQUIDs): principles and performance

**R E Packard**[1] **and Y Sato**[2]
[1] Department of Physics, University of California, Berkeley, California 94720, USA
[2] Rowland Institute at Harvard, Harvard University, Cambridge, Massachusetts 02142, USA

E-mail: rpackard@berkeley.edu, sato@rowland.harvard.edu

**Abstract.** We describe recent progress in developing a superfluid helium analog of the superconducting dc-SQUID. The devices tested thus far are sensitive detectors of rotation as well as useful probes for studies of superfluidity. The key ingredients of the superfluid helium quantum interference device (SHeQUID) involve commercially available technology and modest cryogenic facilities.

The superfluid states of quantum liquids ($^3$He-B and $^4$He) are described by a macroscopic order parameter of the form $\Psi = \sqrt{\rho_s} e^{i\phi}$, where $\rho_s$ is the superfluid density and $\phi$ is the quantum mechanical phase [1]. When two such fluids are coupled together through a small channel, the system exhibits many surprising features. Quintessential phenomena are various Josephson effects, which occur when the channel between the two fluids is sufficiently small. Such a small channel is normally referred to as a weak link or junction. In that scenario, solving the time-dependent Schrodinger's equation applied to the coupled system results in two governing equations:

$$I = I_0 \sin \Delta\phi \tag{1}$$

and

$$\frac{d\Delta\phi}{dt} = -\frac{\Delta\mu}{\hbar} . \tag{2}$$

The first equation (dc Josephson equation [2]) describes the nonlinear relationship between the phase difference across the junction $\Delta\phi$ and the superfluid mass current $I$ through it. The second equation (Josephson-Anderson phase evolution equation [3]) states that the chemical potential difference $\Delta\mu = m(\Delta P / \rho - s\Delta T)$ drives the phase factor to evolve in time. Here $\Delta P$ and $\Delta T$ are pressure and temperature differentials, $\rho$ is the fluid density, $s$ is the entropy per unit mass and $m$ is the mass of constituent particles making up the superfluid, either $^4$He atomic mass or twice the $^3$He mass [1].

The dynamic behaviours predicted by the above two equations are quite counter-intuitive. For example even with the absence of any driving force ($\Delta\mu = 0$), dc mass current could appear across the junction from nonzero $\Delta\phi$. On the other hand, when a constant $\Delta\mu$ is applied across the junction, $\Delta\phi$ evolves linearly in time, resulting in oscillating mass current across the junction. This oscillation phenomenon is called the Josephson oscillation which occurs at frequency $\omega_J \equiv \Delta\mu / \hbar$.

Although electron tunnelling through a thin non-superconducting film constitutes a weak link for superconductors [2], the atomic mass of helium is too large to exhibit appreciable tunnelling. To couple superfluids weakly, one needs the equivalent of a Dayem Bridge [4], a constricted passage whose dimensions are on the order of the superfluid healing length $\xi$. In practice, two reservoirs of superfluid helium can be coupled weakly through an array of apertures. For reasons that are still not obvious the superfluid in an array of weak links behaves coherently with the Josephson oscillations in every aperture being in phase with all the others. An array is required to lift the miniscule mass flow signal above the experimental noise.

For superfluid $^3$He, at zero ambient pressure, the healing length is given by [5]

$$\xi_3 = \frac{65}{(1-T/T_c)^{1/2}} \text{ nm}, \tag{3}$$

where $T_c = 1$ mK is the superfluid $^3$He transition temperature. This characteristic size came within the reach of nanofabrication about 30 years ago. In contrast, the healing length of $^4$He at zero ambient pressure is given by [6]

$$\xi_4 = \frac{0.3}{(1-T/T_\lambda)^{0.67}} \text{ nm}, \tag{4}$$

where $T_\lambda = 2.176$ K is the superfluid $^4$He transition temperature. This sub-nanometer size requirement still remains prohibitive to this day, which explains why the investigations of Josephson effects in superfluids began with $^3$He despite the requirement of mK cryogenics. We show below however that this issue can be circumvented by taking advantage of the diverging temperature dependence of $\xi_4$ near $T_\lambda$.

A flow signature consistent with the $I \propto \sin\Delta\phi$ relation was first reported in 1988 using $^3$He [7], and the Josephson oscillation itself was directly observed a decade later [8]. Figure 1 depicts a generic apparatus similar to the one utilized for the latter experiment. A 65 X 65 array of 90 nm apertures *e*-beam lithographed in a 50 nm-thick silicon nitride membrane was used as a weak link. Fluid motion is hydrodynamically coupled to the diaphragm, which is coated with a superconducting metal. The diaphragm motion is sensed with a Paik-type displacement sensor [9], providing a direct measure of fluid motion in the weak link junction. The application of a step voltage between the diaphragm and the electrode directly above pulls up the diaphragm, creating a pressure difference between the inner and outer reservoirs. This step $\Delta P$ causes the fluid to oscillate across the aperture array, and these Josephson oscillations, whose frequency is proportional to the applied $\Delta P$, are indeed observed.

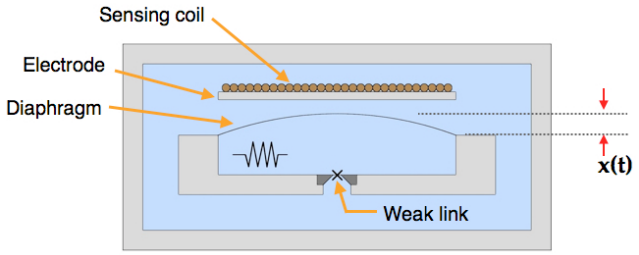


**Figure 1.** Depiction of generic apparatus for investigating superfluid Josephson effects. Electrode and diaphragm form a pressure pump. The SQUID-based transducer monitors the diaphragm position x(t). Weak link is formed by an array of holes. Both $\Delta P$ and $\Delta T$ (induced with the heater depicted) can be used to drive Josephson oscillations.

The superfluid helium quantum interference device (SHeQUID) exploits the Josephson oscillation phenomena discussed above. See figure 2. A torus filled with superfluid helium is interrupted by two weak links. When $\Delta\mu$ is applied across the two junctions, the current oscillates through each junction as $I_{c,1}\sin(\omega_J t)$ and $I_{c,2}\sin(\omega_J t+\Delta\phi_{ext})$, where $\Delta\phi_{ext}$ denotes the phase shift between the two oscillations. The overall amplitude of the total mass current $I_c^*\sin(\omega_J t)$ can be written as

$$I_c^* = (I_{c,1}+I_{c,2})\left\{\cos^2\left(\frac{\Delta\phi_{ext}}{2}\right)+\gamma^2\sin^2\left(\frac{\Delta\phi_{ext}}{2}\right)\right\}^{1/2}, \quad (5)$$

with $\gamma=(I_{c,1}-I_{c,2})/(I_{c,1}+I_{c,2})$. As can be seen in the above relation, the mass current amplitude becomes a function of $\Delta\phi_{ext}$, making the device an interferometer.

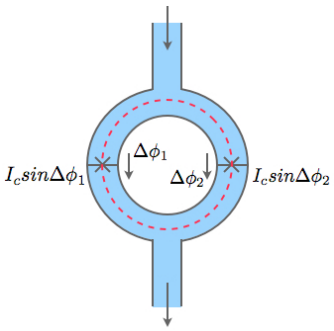


**Figure 2.** SHeQUID configuration. Two junctions are placed in a superfluid torus as in the case of a dc-SQUID. The phase integral condition along the closed loop depicted by a dotted line underlies the interferometry principle.

A SHeQUID is a direct analog of a dc superconducting quantum interference device (dc-SQUID [10]). In the case of a dc-SQUID, the phase shift arises from the magnetic flux through the superconducting loop, rendering the device a very sensitive magnetometer. For a SHeQUID, the role of magnetic flux can be played by various physical phenomena, and one such example is rotation. When the torus as depicted in figure 2 is rotated at speed $\vec{\Omega}$ about an axis perpendicular to its plane, the partitions containing the junctions force the fluid to flow as a solid body. Since superfluid velocity corresponds to phase gradient via $v_s=(\hbar/m)\nabla\phi$ [1], the line integral applied to a closed loop gives $\Delta\phi_{ext}=(2m/\hbar)\vec{\Omega}\cdot\vec{A}$ where $\vec{A}$ is the area vector of the torus. Substituting this into equation 5, one can see that the variation in the amplitude of the combined Josephson oscillation provides information on the rotation of the system.

This rotation-induced phase shift is equivalent to the Sagnac phase shift $\Delta\phi=(2\omega/c^2)\vec{\Omega}\cdot\vec{A}$ seen in optical interferometers where a beam of light is split and recombined while enclosing a finite area [11]. However the phase shift for a given rotation and enclosed area is very different for photons and helium. The induced phase shift is proportional to the effective mass of interfering medium. For a given change in rotation, the resultant signal per device area for a SHeQUID is larger than that for laser interferometers by ten orders of magnitude (ratio of $m_{He}c^2$ to photon energy). This suggests the development of compact sensitive rotation sensors. The first SHeQUID was constructed with $^3$He [12], and its operation was demonstrated by inducing and detecting phase shifts from the rotating Earth.

These developments in $^3$He preceded those in $^4$He by almost two decades. The extremely small size of $^4$He healing length, on the order of a few angstroms, was the primary factor for this delay. As mentioned previously, the healing length diverges near $T_\lambda$. This means that instead of attempting to fabricate sub-nanometer apertures to match the zero-temperature healing length, one could increase the healing length near $T_\lambda$ to match the bigger aperture sizes available. However earlier estimates suggested that the thermally-driven phase fluctuation at 2 K would destroy the temporal coherence of

fluid oscillation in a given aperture [13]. Although this thermal fluctuation is not an issue for $^3$He at its 1mK operating temperature, at a temperature two thousand times higher this was believed to be detrimental to Josephson phenomena in $^4$He. Temperatures so close to $T_\lambda$ also meant significantly diminished superfluid density and hence even smaller signals.

Despite the aforementioned factors, early evidence for $I \propto \sin\Delta\phi$ behaviour in superfluid $^4$He was reported near $T_\lambda$ in 2001 [14], followed by the direct observation of Josephson oscillations four years later [15]. These discoveries and subsequent analysis have suggested that thermal fluctuations may actually be suppressed in an array of apertures due to coupling among them [16]. Another surprise that accompanied these discoveries is that an oscillation phenomenon at the Josephson frequency persists even when the temperature is lowered so that the aperture size is considerably larger than the superfluid healing length [15].

In the regime where the two superfluid reservoirs are strongly coupled, the analysis that leads to equation 1 is no longer valid. When a finite chemical potential difference is applied across an array of holes, superfluid is simply accelerated from one side to the other. The fluid velocity increases until it reaches a critical value, at which point a quantized vortex is stochastically nucleated. The vortex moves across the channel and removes a fixed amount of energy from the fluid flow. The velocity decreases by a fixed amount given by $\Delta v = \kappa / l_{eff}$, where $\kappa = h/m$ is the quantum of circulation and $l_{eff}$ is the effective hydrodynamic length of the aperture. This dissipative event is known as a phase slip [17-20].

When the chemical potential difference persists as in the case of applying and holding $\Delta P$ in an apparatus depicted in figure 1, the process described above repeats, and a series of phase slip events takes place. It can be shown that the frequency for such events happens to be identical to the Josephson frequency. Both the weakly coupled Josephson regime and the strongly coupled phase slip regime have been investigated, and the current-phase relation is seen to change smoothly from linear to sinusoidal as one approaches the transition temperature [21]. It is worthwhile to note that, in the strongly coupled regime, the phase slip events occur synchronously among all the apertures but that degree of synchronicity is observed to decrease as one lowers the temperature further. The nature of the mechanism that synchronizes the array and an explaination of why that synchronization decreases at lower temperatures has been investigated both theoretically and experimentally, [22-24]. However these features are still an unresolved mystery.

**Figure 3.** Multi-turn and gradiometric sensing arm for a SHeQUID. The length of the arm is approximately 0.5m. From Ref [28].

Given the ease of cryogenics at 2 K, many SHeQUIDs have been constructed using $^4$He following the first demonstration of $^4$He SHeQUID in 2006 [25]. As a novel phase gradient meter, it has been utilized to verify the link between the wavefunction picture of superfluid and the Landau's two-fluid model [26]. It has also been used to detect the motion of a quantized vortex and the onset of quantum turbulence [27]. As a compact rotation sensor, the device has seen significant increases in sensitivity. A large area $^4$He SHeQUID with a long multi-turn path in astatic geometry has for example been reported with an intrinsic rotational sensitivity of $1\times10^{-8}$ rad/sec/$\sqrt{\text{Hz}}$ [28]. See figure 3. The total area enclosed is 225 cm$^2$, a forty-fold increase compared to the first $^3$He SHeQUID [12]. The superfluid Josephson system has also formed an ideal test bed for studying some fascinating nonlinear

phenomena such as the Fiske effect, junction size effect, and bifurcation, and those in turn have provided a set of tools to increase the sensitivity and utility of the device [29-32]. For example, flux locking with injected hydrodynamic heat flow for example allows the linearization of the device [33]. A linearized SHeQUID (figure 4) equipped with such function that can operate continuously to automatically measure time-varying rotation rates has been demonstrated in 2013 [34, 35].

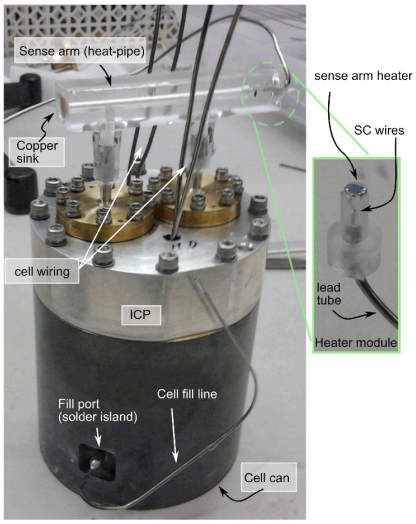


**Figure 4.** Continuously operating, flux-locked SHeQUID. From Ref [35].

The experimental components for the SHeQUID operation have been simplified over the years, and the requirements have become quite modest. For $^4$He SHeQUID experiments, high-resolution thermometers with sub-nK resolution [36, 37] are used to regulate the temperature within several nano-Kelvins of the set point. A recent development involves redesigning these thermometers to utilize the temperature dependence of the magnetic susceptibility of a paramagnetic PdMn alloy [38]. Alloys with the required mixing percentage, Neodymium magnets to apply the external fields, and a dc-SQUID to read out the susceptibility change, can all be purchased commercially. Weaklink arrays are made of approximately 5000 apertures, *e*-beam lithographed in a ~50 nm-thick SiN membrane [39-41]. The aperture diameter depends on experiments, but it typically ranges from 30 nm to 70 nm. This type of aspect ratio is not demanding with the current state-of-the-art nanofabrication, and with a recipe that has been improved upon over the years, the aperture fabrication has even been successfully outsourced [42]. The temperature regime of 2 K is easily obtained, and the experiments have been carried out with simple probes dipped into a liquid $^4$He dewar without a 1 K pot. The whole bath of liquid $^4$He can be temperature controlled to the required precision with minimum liquid loss. With careful engineering [43], it should be feasible to load the experimental stages on cryocoolers to entirely remove the need for a cryogen bath, allowing a remote and fully automated operation.

The proof-of-concept demonstration of the SHeQUID itself as well as various techniques to illuminate and exploit its exotic properties has now been achieved to some extent. As a step towards the next phase for the SHeQUID development as an "instrument", one may explore its untapped sensitivity. The intrinsic device sensitivity is proportional to several parameters including the sensing area, number of apertures in the junctions, and superfluid density. The effects of increasing the sensing area have been studied, and although the signal increase has been reported, this approach has its limitations. Writing the fluid kinetic energy as $LI^2/2$, the superfluid hydrodynamic inductance $L$ can be identified as $(\hbar/m_4)(dI/d\Delta\phi)^{-1}$ [2]. For a sinusoidal current-phase relation of equation 1, this leads to kinetic inductance of the junction (Josephson inductance) $L_J = \hbar/(m_4 I_c)$ at $\Delta\phi = 0$. In contrast for superfluid flowing through the rest of the interfering path of length $l$ and cross sectional area $\sigma$, the inductance is given by $L_t = l/(\rho_s \sigma)$. The device should be designed such that $L_J >> L_t$.

In the case of dc-SQUIDs a separate pickup loop with a large flux capture area can be used while an appropriate impedance matching can be accomplished through flux transformers. In contrast a SHeQUID can only operate in a "bare" circuit because no coupling exists between two loops of neutral superfluid placed nearby. Hence as the interfering path is made significantly long, its hydrodynamic inductance starts to dominate over the Josephson inductance and the device should inevitably start to suffer signal loss. Increasing $\sigma$ to decrease $L_t$ leads to significant fluid volume increase, which could compromise the signal through increased compressibility.

A less complicated route for enhancing sensitivity may be increasing the number of apertures. With *e*-beam lithography and the several hundred micron-size membranes used thus far, a number increase by an order of magnitude is easily feasible. This numerical increase may also have an additional benefit of further suppressing the thermal fluctuations via enhanced coupling. Developing the technique to fabricate even smaller holes is also a fascinating option since that would allow the Josephson regime to extend down to lower temperatures [44]. For example, if operated near 1.5 K, superfluid fraction that contributes to the mass current can be nearly 100 % as opposed to a few % near $T_\lambda$. In principle this should lead to a much higher signal to noise ratio. This approach would require a larger number of apertures to offset the smaller signal per aperture, but with the presence of increased number, this may also have the benefit of suppressed thermal fluctuations. The ultimate phase resolution limit of SheQUIDs may be quantum fluctuations embodied in the uncertainty principle. Assuming that the vibrational noise from the environment can be controlled, it will be critical to suppress thermally excited phase fluctuations if one is to get to that ultimate limit.

Another aspect to consider is a new methodology for detecting the fluid oscillation. The current transduction mechanism relies on the fluid pushing on the diaphragm, with finite spring constant $k$, resulting in a competition between the Josephson energy $(\hbar / m_4)I_c$ and the diaphragm spring energy $k\Delta x^2 / 2$. Rewriting the latter as $k(I_c / \rho A\omega)^2 / 2$, where $A$ is the diaphragm area and $\omega$ is the oscillation frequency and equating the two energies gives the maximum current amplitude that is supportable $I_{c,\max} \sim \hbar\rho^2 A^2\omega^2 / m_4 k$. To increase this upper limit in a given junction, one should use a soft and large diaphragm and operate at high frequencies. While this can be achieved to some extent with the current transducers, a new non-mechanical method to detect the fluid motion in the junctions could remove the dependence on hydrodynamic coupling, which is naturally a step-down transformer. Similarly, since the fluid oscillation occurs in the velocity domain, the signal obtained with the displacement sensor diminishes as the frequency increases. A sensitive sensor whose output is proportional to velocity instead of displacement could provide the means to take full advantage of the increased signal.

Ultrasensitive rotation sensors find applications in multidisciplinary fields including geodesy, geophysics, inertial navigation, and seismology. With the device technology rapidly developing, it is not at all inconceivable to use SHeQUIDs to complement state-of-the-art ring laser gyroscopes in their quest to test general relativistic effects on Earth [45]. Furthermore, due to their novel ability to detect quantum mechanical phase differences, SHeQUIDs may also be utilized as tools for studying various Berry's phase phenomena. For example, He-McKeller-Wilkens topological phase was recently observed with atom interferometers [46-49].

During the past decade many of the Josephson effects discovered with superfluid helium have also been detected in cold BEC gases [50-52]. Several laboratories are pursuing the development of these matter wave interferometers [53, 54]. In these projects it is a distinct advantage to be working with essentially room temperature elements rather than cryostats. However phase fluctuations limited by the finite number of atoms and the inability to easily produce large enclosed area may limit the cold atom devices. With so much effort now underway the future is bound to be interesting both for SHeQUIDs and their cold atom counterparts.

More details related to SHeQUIDs can be found in Ref [55]. For discussion on superfluid gyroscopes based on a single weaklink and a large parallel path, see Ref [56].

This work has been supported by the NSF Division of Materials Research and the Rowland Institute at Harvard.

**References**

[1] Tilley D R and Tilley J 1990 *Superfluidity and Superconductivity* (Bristol: Institute of Physics)
[2] Likharev K K 1986 *Dynamics of Josephson Junctions and Circuits* (New York: Academic Press)
[3] Anderson P W 1966 *Rev. Mod. Phys.* **38** 298
[4] Anderson P W and Dayem A H 1964 *Rev. Rev. Lett.* **13** 195
[5] Vollhardt D and Wolfle P 1990 *The Superfluid Phases of Helium-3* (New York: Taylor and Francis)
[6] Henkel R P, Smith E N and Reppu J D 1969 *Rev. Rev. Lett.* **23** 1276
[7] Avenel O and Varoquaux E 1988 *Phys. Rev. Lett.* **60** 416
[8] Pereverzev S V, Loshak A, Backhaus S, Davis J C and Packard R E 1997 *Nature* **388** 449
[9] Paik H 1976 *J. Appl. Phys.* **47** 1168
[10] Clarke J and Braginski A I 2004 The *SQUID Handbook: Fundamentals and Technology of SQUIDs and SQUID Systems* (Weinheim: Wiley-VCH)
[11] Post E J 1967 *Rev. Mod. Phys.* **39** 475
[12] Simmonds R, Marchenkov A, Hoskinson E, Davis J C and Packard R E 2001 *Nature* **412** 55
[13] Zimmermann W 1987 *in Proceedings of the Fifth Oregon Conference on Liquid Helium, a Report from the Department of Physics, University of Oregon*, p 118
[14] Sukhatme K, Mukharsky Y, Chui T and Pearson D 2001 *Nature* **411** 280
[15] Hoskinson E, Packard R E and Haard T 2005 *Nature* **433** 376
[16] Chui T, Holmes W and Penanen K 2003 *Phys. Rev. Lett.* **90** 085301
[17] Onsagar L 1949 *Nuovo Cimento* **6** 249
[18] Feynman R P 1955 *Progress on Low Temperature Physics* edited by Gorter CJ (Amsterdam: North-Holland) vol 1 ch 2
[19] Anderson P W 1966 *Quantum Fluids* edited by Brewer D F (Amsterdam: North-Holland) p 146
[20] Avenel O and Varoquaux E 1985 *Phys. Rev. Lett.* **55** 2704
[21] Hoskinson E, Sato Y, Hahn I and Packard R E 2005 *Nat. Phys.* **2** 23
[22] Sato Y, Hoskinson E and Packard R E 2006 *Phys. Rev. B* **74** 144502
[23] Sato Y, Hoskinson E and Packard R E 2007 *JLTP* **149** 222
[24] Pekker D, Barankov R and Goldbart P M 2007 *Phys. Rev. Lett.* **98** 175301
[25] Hoskinson E, Sato Y and Packard R E 2006 *Phys. Rev. B* **74** 100509(R)
[26] Sato Y, Joshi A and Packard R E 2007 *Phys. Rev. Lett.* **98** 195302
[27] Sato Y, Joshi A and Packard R E 2007 *Phys. Rev. B* **76** 052505
[28] Narayana S and Sato Y 2011 *Phys. Rev. Lett.* **106** 255301
[29] Narayana S and Sato Y 2010 *Phys. Rev. Lett.* **105** 205302
[30] Hoskinson E, Sato Y, Penanen K and Packard R E 2006 *AIP Conf.* **850** 117
[31] Sato Y 2010 *Phys. Rev. B* **81** 172502
[32] Narayana S and Sato Y 2011 *Phys. Rev. Lett.* **106** 055302
[33] Sato Y, Joshi A and Packard R E 2007 *Appl. Phys. Lett.* **91** 074107
[34] Joshi A and Packard R E 2013 *JLTP* **172** 162
[35] Joshi A, 2013 Ph.D. thesis. University of California at Berkeley
[36] Welander P B and Hahn I 2001 *Rev. Sci. Instr.* **72** 3600
[37] Welander P, Barmatz M and Hahn I 2000 *IEEE Trans. Instr. Meas.* **49** 253
[38] Narayana S and Sato Y 2010 *IEEE Trans. Appl. Supercond.* **20** 2402
[39] Amar A, Lozes R, Sasaki Y, Davis J C and Packard R E 1993 *J. Vac Sci. Technol. B* **11** 259
[40] Loshak A 1999 Ph.D. thesis. University of California at Berkeley 2007
[41] Joshi A, Sato Y and Packard R E 2009 *J. Phys. Conf. Ser.* **150** 012018
[42] EigenPhase Technologies, Trumansburg, NY 14886

[43] Pelliccione M, Sciambi A, Bartel J, Keller A J and Goldhaber-Gordon D 2013 *Rev. Sci. Instr.* **84** 033703
[44] Murakawa S, Chikazawa Y, Higashino R, Yoshimura K, Shibayama Y, Kuriyama K, Honda K, and Shirahama K 2010 *International Symposium on Quantum Fluids and Solids* PS1-27
[45] Schreiber K U and Wells J P R 2013 *Rev. Sci. Instr.* **84** 041101
[46] Lepoutre S, Gauguet A, Trenec G, Bucher M and Vigue J 2012 *Phys. Rev. Lett.* **109** 120404
[47] He XG and McKellar B H J 1993 *Phys. Rev. A* **47** 3424
[48] Wei H, Han R and Wei X 1995 *Phys. Rev. Lett.* **75** 2071
[49] Sato Y and Packard R E 2009 *J. Phys. Conf. Ser.* **150** 32093
[50] Albiez M, Gati R, Folling J, Hunsmann S, Cristiani M and Oberthaler M 2005 *Phys. Rev. Lett.* **95** 010402
[51] Levy S, Lahoud E, Shomroni I and Steinhauer J 2007 *Nature* **449** 579
[52] Eckel S, Lee J G, Jendrzejewski F, Murray N, Clark C W, Lobb C J, Phillips W D, Edwards M and Campbell G K 2014 *Nature* **506** 200
[53] Wright K C, Blakestad R B, Lobb C J, Phillips W D and Campbell G K 2013 *Phys. Rev. Lett.* **110** 025302
[54] Ryu C, Blackburn P W, Blinova A A and Boshier M G 2013 *Phys. Rev. Lett.* **111** 205301
[55] Sato Y and Packard R E 2012 *Rep. Prog. Phys.* **75** 016401
[56] Avenel O, Mukharsky Y and Varoquaux E 2004 *JLTP* **135** 745